NEGF Modeling of Carrier Transport in Antimonide-based Type-II Superlattice Absorbers

NEGF Modeling of Carrier Transport in Antimonide-based Type-II Superlattice Absorbers

F. Bertazzi[1,2], **A. Tibaldi**[1], **J. A. Gonzalez Montoya**[1], **M. Goano**[1,2], **and E. Bellotti**[3]

[1]Dipartimento di Elettronica e Telecomunicazioni, Politecnico di Torino
Corso Duca degli Abruzzi 24, Torino 10129, Italy
[2]Istituto di Elettronica e di Ingegneria dell'Informazione e delle Telecomunicazioni (IEIIT)
Consiglio Nazionale delle Ricerche (CNR), Corso Duca degli Abruzzi 24, Torino 10129, Italy
[3]Department of Electrical and Computer Engineering, Boston University
8 Saint Mary's Street, Boston, Massachusetts 02215, USA

Abstract— Aiming at a rigorous description of optical absorption and carrier transport in broken-gap type-II superlattice absorbers, we employ a quantum-kinetic framework based on a nonequilibrium Green's function approach, with fully nonlocal carrier-phonon and carrier-photon self-energies computed within the self-consistent Born approximation. For a realistic description of the electronic structure, we express Green's functions and self-energies in a multiband multiband $k \cdot p$ basis within the envelope function approximation. We address the staggering cost of multiband NEGF models by transforming the kinetic equations from real space to a modal space spanned by numerically generated problem-matched basis functions. Inspection of energy- and position-resolved single particle properties such as carrier density and spectral current offers insight into the complex nature of carrier transport in broken-gap nanostructures.

1. INTRODUCTION

The nearly lattice-matched InAs/GaSb/AlSb family offers a viable alternative to the state-of-the-art bulk HgCdTe-based infrared imaging technology [1–5]. The flexibility in controlling the energy gap through adjustment of the constituent layer compositions and thicknesses, the attainable tuning of the infrared detection wavelength over most of the technologically-relevant infrared spectrum, the possibility of even realizing different energy-band alignments from type-I to type-II broken-gap (misaligned, or type-III) heterostructures, have led to the development of new device concepts and architectures [6] with potentially suppressed Auger generation rates, lower dark currents and higher operating temperature. As the promise of improved performance of type-II superlattices (T2SLs) has not yet been fully realized, mainly because of the short SRH lifetimes, theoretical investigations are needed to understand the fundamental limits of these devices. T2SL modeling requires a genuine quantum approach to describe different transport regimes, e.g., miniband transport in the absorbing region and Wannier-Stark hopping in carrier relaxation layers [7]. A realistic description of the electronic structure, including the evanescent states in the gap is needed for the description of interband tunneling. Besides providing carrier transport, the superlattice states also mediate optical absorption through spatially indirect transitions.

2. THEORY AND RESULTS

Our non-equilibrium Green's function (NEGF) code includes acoustic scattering in the equipartition approximation, inelastic polar optical scattering, impurity scattering, and carrier-photon scattering. All self-energies are fully nonlocal and computed in the self-consistent Born approximation (SCBA), see [8–10]. The electronic structure of T2SLs has been described using a variety of theoretical approaches such as the empirical tight-binding method [11], the empirical pseudopotential method [12], and multiband $k \cdot p$ models within the envelope function approximation [13–15]. With the inclusion of the first conduction band, heavy-hole, light-hole, and spin-orbit split-off bands, the multiband 8×8 $k \cdot p$ model seems a good compromise between accuracy and computational efficiency. We apply the axial approximation so that the band structure depends only on the magnitude of the transverse wavevector, which simplifies the numerical integration of the self-energies. Under axial approximation, the bulk Hamiltonian block-diagonalizes with respect to the spin-coordinates (i.e., the 8×8 Hamiltonian decouples in two 4×4 matrices) [16, 17]. $k \cdot p$ parameters can be derived from full-Brilluoin-zone band structure calculations [18], but here we adopt the fitting parameters reported in [16]. We transform the generalized eigenvalue problem

formulated in a finite-element overlapping basis to a standard eigenvalue problem in symmetrically orthogonalized functions by means of Löwdin symmetric orthogonalization, which eliminates the complication of having different contravariant and covariant representations for Green's functions and self-energies.

Even with the approximations discussed above, the NEGF approach remains challenging from the computational standpoint. Inspired by the spectral decomposition of the Green's function, the idea behind reduced order-models (in this context also known as mode space or low rank approaches), is to transform the problem from the original real space to a modal space spanned by few problem-matched basis functions [19]. These basis functions can be obtained, for example, by selecting the eigenstates of the noninteracting Hamiltonian (i.e., without boundary and scattering self-energies) with energies within a given energy range (referred in the following as *near* states). In practice this range should include all the relevant conduction channels of the conduction/valence bands of the nanodevice. In this representation, the number of required basis functions is much less than the original space, which allows to reduce the computational burden significantly. Reduced-order models are usually limited to the coherent limit, since the extension to the dissipative case requires the self-energies to be computed directly in the reduced-order subspace. One way to include scattering without losing the computational advantage is to obtain localized basis functions by diagonalizing the position operator in the reduced-order representation [20]. For a field-periodic periodic structure, e.g., quantum cascade lasers, this procedure leads to the definition of maximally localized Wannier functions [21]. The Dyson and Keldish equations are then projected in the reduced-order subspace spanned by the localized basis functions. Since every localized basis function is associated with the corresponding position eigenvalue, the scattering self-energies can be discretized directly in the mode space representation. In order to avoid current fluctuations due to the incomplete representation of the boundary self-energies [20], we compute the boundary self-energies in mode space by folding the influence of the *remote* states into the near states. The NEGF algorithm proceeds as usual, the scattering self-energies are computed directly in the reduced-order mode space. As the eigenstates of the position operator are not energy eigenstates of the nanostructure, the interpretation of the results in the reduced-order space is difficult. Therefore, once self-consistency is achieved between Green's functions and self-energies, the scattering self-energies are transformed back to real space, and the Dyson and Keldish equations are solved in real space to obtain the relevant one-particle properties.

Preliminary results for a type-II InAs/GaSb superlattice absorber illuminated with monochromatic light and terminated with selective contacts are shown in Fig. 1. Upon convergence, the total energy-integrated current is conserved over the whole device region (this is a very stringent test for any NEGF model). The continuous stripes in the current spectrum, see Fig. 1(a), are

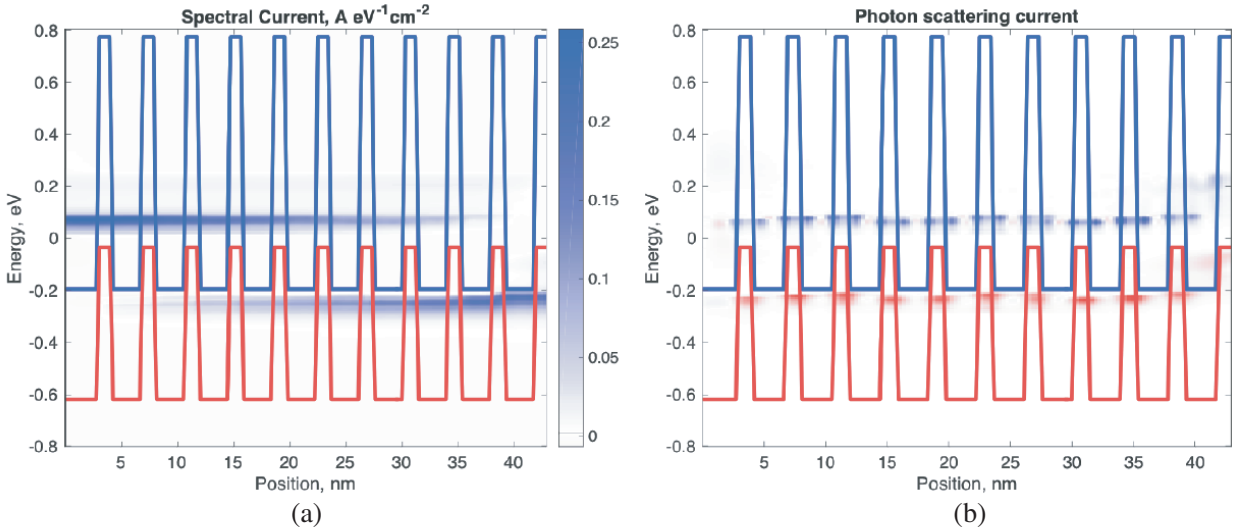

(a) (b)

Figure 1: (a) Spatially resolved photocurrent spectrum under monochromatic illumination of $100\,\mathrm{W/m^2}$ with $E_\gamma = 0.3\,\mathrm{eV}$, with carrier selective contacts. (b) Divergence of the photon scattering current, showing the spatial and energy distribution of the photogenerated carriers: positive values (blue specks) correspond to in-scattering of electrons in the conduction band and to outscattering of holes in the valence band.

indicative of miniband transport of electrons and holes towards their corresponding contacts. Since the self-energies are additive, one can separate their contribution to the total current (this is just an approximation, of course, because Green's functions determine self-energies and viceversa). The divergence of the phonon scattering current shows the optical transitions between the localized holes in the GaSb layers and the electron miniband, Fig. 1(b).

ACKNOWLEDGMENT

This work was supported by the U.S. Army Research Laboratory through the Collaborative Research Alliance (CRA) for MultiScale multidisciplinary Modeling of Electronic materials (MSME). Computational resources were provided by HPC@POLITO, a project of Academic Computing within the Department of Control and Computer Engineering at the Politecnico di Torino (http://www.hpc.polito.it).

REFERENCES

1. Rogalski, A., *Infrared Detectors*, 2nd Edition, CRC Press, Boca Raton, FL, 2011.
2. Kinch, M. A., *State-of-the-Art Infrared Detector Technology*, SPIE, Bellingham, WA, 2014.
3. Vallone, M., M. Mandurrino, M. Goano, F. Bertazzi, G. Ghione, W. Schirmacher, S. Hanna, and H. Figgemeier, "Numerical modeling of SRH and tunneling mechanisms in high-operating-temperature MWIR HgCdTe photodetectors," *J. Electron. Mater.*, Vol. 44, No. 9, 3056–3063, 2015.
4. Vallone, M., M. Goano, F. Bertazzi, G. Ghione, W. Schirmacher, S. Hanna, and H. Figgemeier, "Comparing FDTD and ray tracing models in the numerical simulation of HgCdTe LWIR photodetectors," *J. Electron. Mater.*, Vol. 45, No. 9, 4524–4531, 2016.
5. Rogalski, A., P. Martyniuk, and M. Kopytko, "InAs/GaSb type-II superlattice infrared detectors: Future prospect," *Appl. Phys. Rev.*, Vol. 4, No. 3, 031304, 2017.
6. Sood, A. K., J. W. Zeller, R. E. Welser, Y. R. Puri, N. K. Dhar, P. S. Wijewarnasuriya, and S. Krishna, "Design and development of two-dimensional strained layer superlattice (SLS) detector arrays for IR applications," *Two-dimensional Materials for Photodetector*, P. K. Nayak, Ed., Ch. 5, 103–138, IntechOpen, Rijeka, Croatia, 2018.
7. Tian, Z., R. T. Hinkey, R. Q. Yang, D. Lubyshev, Y. Qiu, J. M. Fastenau, W. K. Liu, and M. B. Johnson, "Interband cascade infrared photodetectors with enhanced electron barriers and p-type superlattice absorbers," *J. Appl. Phys.*, Vol. 111, No. 8, 024510, 2012.
8. Steiger, S., "Modelling nano-LEDs," Ph.D. dissertation, Eidgenössische Technische Hochschule Zürich, 2009.
9. Aeberhard, U., "A microscopic theory of quantum well photovoltaics," Ph.D. dissertation, Eidgenössische Technische Hochschule Zürich, 2008.
10. Aeberhard, U., "Photovoltaics at the mesoscale: Insights from quantum-kinetic simulation," *J. Phys. D*, Vol. 51, No. 32, 323002, 2018.
11. Wei, Y. and M. Razeghi, "Modeling of type-II InAs/GaSb superlattices using an empirical tight-binding method and interface engineering," *Phys. Rev. B*, Vol. 69, No. 8, 085316, 2004.
12. Magri, R. and A. Zunger, "Effects of interfacial atomic segregation and intermixing on the electronic properties of InAs/GaSb superlattices," *Phys. Rev. B*, Vol. 65, No. 16, 165302, 2002.
13. Klipstein, P. C., "Operator ordering and interface-band mixing in the Kane-like Hamiltonian of lattice-matched semiconductor superlattices with abrupt interfaces," *Phys. Rev. B*, Vol. 81, No. 23, 235314, 2010.
14. Livneh, Y., P. C. Klipstein, O. Klin, N. Snapi, S. Grossman, A. Glozman, and E. Weiss, "$k \cdot p$ model for the energy dispersions and absorption spectra of InAs/GaSb type-II superlattices," *Phys. Rev. B*, Vol. 86, No. 23, 235311, 2012.
15. Livneh, Y., P. C. Klipstein, O. Klin, N. Snapi, S. Grossman, A. Glozman, and E. Weiss, "Erratum: $k \cdot p$ model for the energy dispersions and absorption spectra of InAs/GaSb type-II superlattices," *Phys. Rev. B*, Vol. 90, No. 3, 039903, 2014.
16. Qiao, P.-F., S. Mou, and S. L. Chuang, "Electronic band structures and optical properties of type-II superlattice photodetectors with interfacial effect," *Opt. Express*, Vol. 20, No. 2, 2319–2334, 2012.
17. Liu, G. and S.-L. Chuang, "Modeling of Sb-based type-II quantum cascade lasers," *Phys. Rev. B*, Vol. 65, No. 16, 165220, 2002.

18. Zhou, X., F. Bertazzi, M. Goano, G. Ghione, and E. Bellotti, "Deriving $k \cdot p$ parameters from full-Brillouin-zone descriptions: A finite-element envelope function model for quantum-confined wurtzite nanostructures," *J. Appl. Phys.*, Vol. 116, No. 3, 033709, Jul. 2014.
19. Bertazzi, F., O. A. Peverini, M. Goano, G. Ghione, R. Orta, and R. Tascone, "A fast reduced-order model for the full-wave FEM analysis of lossy inhomogeneous anisotropic waveguides," *IEEE Trans. Microwave Theory Tech.*, Vol. 50, No. 9, 2108–2114, Sep. 2002.
20. Zeng, L., Y. He, M. Povolotskyi, X. Liu, G. Klimeck, and T. Kubis, "Low rank approximation method for efficient Green's function calculation of dissipative quantum transport," *J. Appl. Phys.*, Vol. 113, No. 21, 213707, 2013.
21. Lee, S.-C. and A. Wacker, "Nonequilibrium Green's function theory for transport and gain properties of quantum cascade structures," *Phys. Rev. B*, Vol. 66, No. 24, 245314, 2002.